

Evidence for a new $SU(4)$ symmetry with $J = 2$ mesons

M. Denissenya,^{1,*} L. Ya. Glozman,^{1,†} and M. Pak^{1,‡}

¹*Institut für Physik, FB Theoretische Physik, Universität Graz, Universitätsplatz 5, 8010 Graz, Austria*

Recently, a new symmetry of mesons has been found upon truncation of the quasi-zero modes of the Overlap Dirac operator in lattice simulations. Namely, the $\rho, \rho', \omega, \omega', a_1, b_1, h_1$ and possibly f_1 $J = 1$ mesons get degenerate after removal of the quasi-zero modes. This emergent symmetry has been established to be $SU(4) \supset SU(2)_L \times SU(2)_R \times U(1)_A$. It is higher than the symmetry of the QCD Lagrangian and provides not only a mixing of quarks of given chirality in the isospin space, but also the mixing of left-handed and right-handed components. Here we study, with the Overlap Dirac operator, the isovector $J = 2$ mesons upon the quasi-zero mode reduction and observe a similar degeneracy. This result further supports the $SU(4)$ symmetry in mesons of given spin $J \geq 1$.

PACS numbers: 12.38Gc, 11.25.-w, 11.30.Rd

I. INTRODUCTION

In recent $N_F = 2$ dynamical lattice simulations with the Overlap Dirac operator a large degeneracy of the spin $J = 1$ $\rho, \rho', \omega, \omega', a_1, b_1, h_1$ and possibly f_1 mesons has been discovered upon removal of the lowest-lying eigenmodes of the Dirac operator from the valence quark propagators [1, 2]¹. The correlators have demonstrated a clean exponential decay suggesting that the mesons survive this truncation.

One expects a priori, that upon elimination of the quasi-zero modes of the Dirac operator, the chiral symmetry should be restored, since the quark condensate of the vacuum is connected with the density of the quasi-zero modes via the Banks-Casher relation [5]. However, it has turned out that not only degeneracy patterns from the $SU(2)_L \times SU(2)_R$ and $U(1)_A$ symmetries are observed, but a larger degeneracy that includes all possible chiral multiplets for $J = 1$ mesons. This symmetry has been established to be $SU(4) \supset SU(2)_L \times SU(2)_R \times U(1)_A$ that includes both the isospin rotations of quarks of given chirality as well as the rotations of chirality itself (chiralspin rotations) [6, 7].

The $SU(4)$ symmetry is higher than the $SU(2)_L \times SU(2)_R \times U(1)_A$ symmetry of the QCD Lagrangian and should be consequently considered as an emergent symmetry that reflects the QCD dynamics in $J = 1$ mesons without the quasi-zero modes of the Dirac operator. This symmetry implies the absence of the color-magnetic field in the system and might be interpreted as a manifestation of the dynamical QCD string.

In the present paper we study the isovector $J = 2$ mesons upon the reduction of the lowest-lying eigenmodes from the Overlap valence quark propagators. We obtain the same symmetry patterns as for $J = 1$ mesons,

which supports consequently the existence of the $SU(4)$ symmetry in $J \geq 1$ mesons after the quasi-zero mode reduction.

The structure of the article is as follows: In Chapter II we discuss the parity-chiral, chiralspin and $SU(4)$ multiplets for the tensor mesons and respective interpolators and our expectations for the truncation of the lowest-lying Dirac eigenmodes. In Chapter III we describe the lattice technicalities. The results are presented in Chapter IV. Conclusions are given in Chapter V. Additional tables are provided in Appendix A.

II. THEORETICAL PREDICTIONS FOR THE LOW-MODE REMOVAL

We discuss the theoretical predictions for the tensor meson spectrum after low-mode removal, which come either from the $SU(2)_L \times SU(2)_R$ and $U(1)_A$ restorations Refs. [8, 9], or from the higher $SU(4)$ symmetry, Refs. [6, 7]. We also present interpolators with the respective symmetry transformation properties.

A. Chiral symmetry predictions

In Fig. 1 we show the classification of tensor mesons according to the parity-chiral group $SU(2)_L \times SU(2)_R \times \mathcal{C}_i$, with \mathcal{C}_i denoting the parity group.

In a situation, where the $SU(2)_L \times SU(2)_R$ chiral symmetry is restored but no higher symmetry is present, only mesons within each parity-chiral multiplet r must be degenerate. For instance, in $(1, 0) \oplus (0, 1)$ the a_2 and ρ_2 states, which are related via $SU(2)_A$ should have the same mass². If $U(1)_A$ is restored as well, all four mesons in the $(1/2, 1/2)_a$ and $(1/2, 1/2)_b$ representations should be mass degenerate, *i.e.* the $SU(2)_L \times SU(2)_R \times U(1)_A$

* mikhail.denissenya@uni-graz.at

† leonid.glozman@uni-graz.at

‡ markus.pak@uni-graz.at

¹ A hint for this symmetry has been seen earlier with the Chirally Improved Dirac operator [3]; for a previous lattice study on the low-mode truncation see Ref. [4].

² $SU(2)_A$ is the shorthand notation for the axial part of the $SU(2)_L \times SU(2)_R$ transformations.

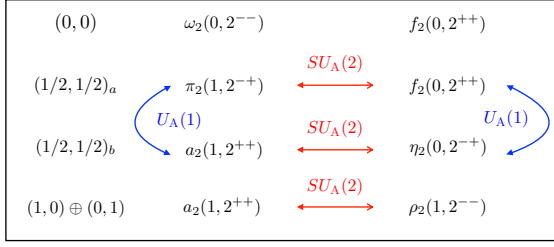


Figure 1: On the left row the irreducible representations r of $SU(2)_L \times SU(2)_R \times C_i$ are given. Each meson is denoted as (I, J^{PC}) , with I isospin, J total angular momentum, P parity and C charge conjugation. The $SU(2)_A$ and $U(1)_A$ connections are denoted by red and blue lines, respectively.

restoration requires the following degeneracies ³

$$\pi_2 \longleftrightarrow f_2 \longleftrightarrow a'_2 \longleftrightarrow \eta_2, \quad (1)$$

and

$$a_2 \longleftrightarrow \rho_2. \quad (2)$$

The states from the singlet $(0,0)$ representations are invariant with respect to both $SU(2)_L \times SU(2)_R$ and $U(1)_A$ transformations and consequently these symmetries do not constrain their masses.

One of the most interesting features of the parity-chiral group, Fig. 1, is, that two independent 2^{++} isovector, a_2, a'_2 , and two independent 2^{++} isoscalar, f_2, f'_2 , mesons must exist. They differ from each other by the content of left- and right-handed quarks and therefore by the chiral representation r . They are not connected via a $SU(2)_L \times SU(2)_R$ or $U(1)_A$ transformation, so their masses should be different without additional symmetry constraints. If their masses are degenerate, then there is a symmetry connecting the states of Eq. (1) with the states of Eq. (2). Hence, in such a situation a larger symmetry than $SU(2)_L \times SU(2)_R \times U(1)_A$ has to be present. This issue will be discussed in the next subsection.

In Table I we classify the interpolators \mathcal{O}_i used in our lattice study into the irreducible representations r of the parity-chiral group.

B. Predictions from $SU(4)$

The states and interpolators from the $(1/2, 1/2)_a$ and $(1/2, 1/2)_b$ representations have the $\bar{L}R \pm \bar{R}L$ chiral content, while the states (interpolators) from the $(0,0)$ and $(1,0) \oplus (0,1)$ representations contain the $\bar{L}L \pm \bar{R}R$ quark

³ The a_2 meson in $(1/2, 1/2)_b$ is here denoted as a'_2 , to distinguish it from the a_2 meson in $(1,0) \oplus (0,1)$. The same is true for the f_2 meson, which in $(1/2, 1/2)_a$ is denoted as f'_2 to distinguish it from the f_2 in $(0,0)$.

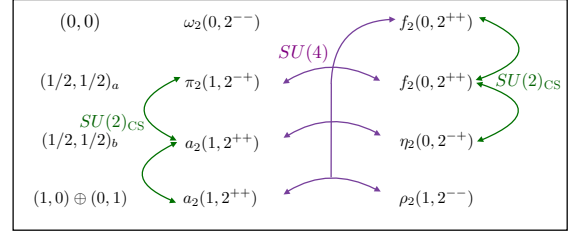


Figure 2: The $SU(2)_{CS}$ triplets are denoted by green lines; ω_2 and ρ_2 mesons are $SU(2)_{CS}$ singlets. The $SU(4)$ 15-plet is indicated by purple lines; ω_2 is the $SU(4)$ singlet.

combinations. A symmetry that can connect these representations is the $SU(2)_{CS}$ (chiral spin) rotation [6, 7]. The rotations in an imaginary chiralspin space mix left- and right-handed components of quarks of given flavor. The $SU(2)_{CS}$ triplets and singlets of quarks are shown in Fig. 2. The $U(1)_A$ symmetry is a subgroup of the $SU(2)_{CS}$.

When we combine both $SU(2)_L \times SU(2)_R$ and $SU(2)_{CS}$ symmetries we arrive at a $SU(4)$ group with the fundamental vector

$$\Psi = \begin{pmatrix} u_L \\ u_R \\ d_L \\ d_R \end{pmatrix}, \quad (3)$$

[6, 7]. The $SU(4)$ transformations mix both quarks of different flavors and different chiralities. The irreducible representations of $SU(4)$ for $\bar{q}q$ systems are a singlet and a 15-plet. The 15-plet includes the following mesons

$$f_2 \longleftrightarrow f'_2 \longleftrightarrow \pi_2 \longleftrightarrow a_2 \longleftrightarrow a'_2 \longleftrightarrow \eta_2 \longleftrightarrow \rho_2, \quad (4)$$

and the singlet is ω_2 , see Fig. 2. All the states from the 15-plet must be mass-degenerate. To observe the $SU(4)$ symmetry it is sufficient, however, to see at the same time the degeneracy of one of the chiral multiplets and of one of the $SU(2)_{CS}$ triplets. For this purpose it is sufficient to study, e.g., all possible isovector mesons ρ_2, a_2, a'_2, π_2 .

III. LATTICE TECHNICALITIES

A. Gauge Field Configurations

We use two-flavor dynamical Overlap fermion gauge field configurations on a $16^3 \times 32$ lattice with lattice spacing $a \sim 0.12$ fm generated and generously provided by the JLQCD collaboration, Refs. [11, 12]. The pion mass is $M_\pi = 289(2)$ MeV, Ref. [13]. The topological sector is fixed to $Q_T = 0$. Our gauge ensemble consists of 83 gauge configurations.

I, J^{PC}	\mathcal{O}	r	O_h
$\rho_2(1, 2^{--})$	$Q_{ijk}\bar{a}_{\partial_k}\gamma_j\gamma_5b_n - Q_{ijk}\bar{a}_n\gamma_j\gamma_5b_{\partial_k}$	$(1, 0) \oplus (0, 1)$	E
	$Q_{ijk}\bar{a}_{\partial_k}\gamma_j\gamma_5b_w - Q_{ijk}\bar{a}_w\gamma_j\gamma_5b_{\partial_k}$		
	$ \epsilon_{ijk} \bar{a}_{\partial_k}\gamma_j\gamma_5b_n - \epsilon_{ijk} \bar{a}_n\gamma_j\gamma_5b_{\partial_k}$	$(1, 0) \oplus (0, 1)$	T_2
	$ \epsilon_{ijk} \bar{a}_{\partial_k}\gamma_j\gamma_5b_w - \epsilon_{ijk} \bar{a}_w\gamma_j\gamma_5b_{\partial_k}$		
$a_2(1, 2^{++})$	$Q_{ijk}\bar{a}_{\partial_k}\gamma_jb_n - Q_{ijk}\bar{a}_n\gamma_jb_{\partial_k}$	$(1, 0) \oplus (0, 1)$	E
	$Q_{ijk}\bar{a}_{\partial_k}\gamma_jb_w - Q_{ijk}\bar{a}_w\gamma_jb_{\partial_k}$		
	$Q_{ijk}\bar{a}_{\partial_k}\gamma_j\gamma_t b_n - Q_{ijk}\bar{a}_n\gamma_j\gamma_t b_{\partial_k}$	$(1/2, 1/2)_b$	T_2
	$Q_{ijk}\bar{a}_{\partial_k}\gamma_j\gamma_t b_w - Q_{ijk}\bar{a}_w\gamma_j\gamma_t b_{\partial_k}$		
	$ \epsilon_{ijk} \bar{a}_{\partial_k}\gamma_jb_n - \epsilon_{ijk} \bar{a}_n\gamma_jb_{\partial_k}$	$(1, 0) \oplus (0, 1)$	
	$ \epsilon_{ijk} \bar{a}_{\partial_k}\gamma_jb_w - \epsilon_{ijk} \bar{a}_w\gamma_jb_{\partial_k}$		
$\pi_2(1, 2^{-+})$	$ \epsilon_{ijk} \bar{a}_{\partial_k}\gamma_j\gamma_t b_n - \epsilon_{ijk} \bar{a}_n\gamma_j\gamma_t b_{\partial_k}$	$(1/2, 1/2)_b$	T_2
	$ \epsilon_{ijk} \bar{a}_{\partial_k}\gamma_j\gamma_t b_w - \epsilon_{ijk} \bar{a}_w\gamma_j\gamma_t b_{\partial_k}$		
	$Q_{ijk}\bar{a}_{\partial_k}\gamma_j\gamma_t\gamma_5b_n - Q_{ijk}\bar{a}_n\gamma_j\gamma_t\gamma_5b_{\partial_k}$	$(1/2, 1/2)_a$	
	$Q_{ijk}\bar{a}_{\partial_k}\gamma_j\gamma_t\gamma_5b_w - Q_{ijk}\bar{a}_w\gamma_j\gamma_t\gamma_5b_{\partial_k}$		
$\rho(1, 1^{--})$	$\bar{a}_n\gamma_jb_n$	$(1, 0) \oplus (0, 1)$	T_1
	$\bar{a}_w\gamma_jb_w$		
	$\bar{a}_n\gamma_j\gamma_t b_n$	$(1/2, 1/2)_b$	
$a_1(1, 1^{++})$	$\bar{a}_w\gamma_j\gamma_t b_w$		
	$\bar{a}_n\gamma_j\gamma_5b_n$	$(1, 0) \oplus (0, 1)$	
	$\bar{a}_w\gamma_j\gamma_5b_w$		
$b_1(1, 1^{+-})$	$\bar{a}_n\gamma_j\gamma_t\gamma_5b_n$	$(1/2, 1/2)_a$	
	$\bar{a}_w\gamma_j\gamma_t\gamma_5b_w$		

Table I: List of tensor and vector meson interpolators \mathcal{O} classified with respect to the chiral representations r and to the irreducible representations E, T_2 of the hyper-cubic group O_h . The interpolators are defined in accordance with Ref. [10]; n and w denote two different smearing widths of the quark sources.

B. Source smearing

In the previous studies of $J = 1$ mesons, Refs. [1, 2], we have used quark propagators with stochastic sources generated by the JLQCD collaboration. The spin $J = 2$ mesons require quark propagators with derivatives, however. Given the JLQCD gauge configurations we calculate the quark propagators using our standard techniques with different smearing widths of Gaussian type [14]. A set of different extended sources with different smearing widths allows for a larger operator basis in the variational method.

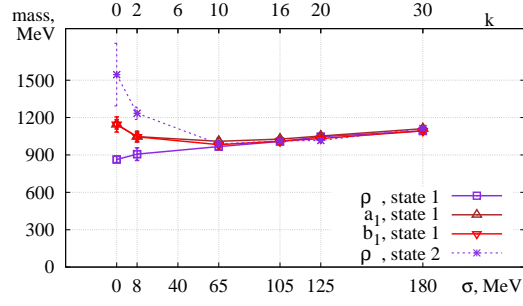
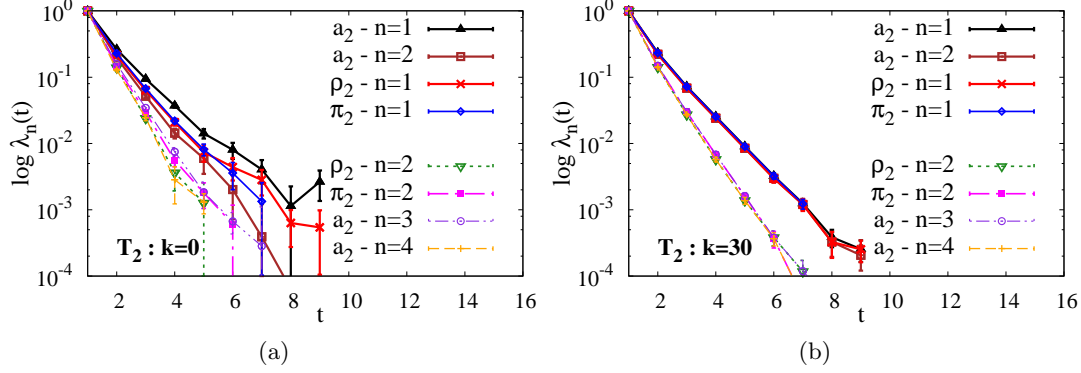
Gaussian smearing has two parameters, the hopping parameter κ and the number of smearing steps N . It produces Gaussian shaped covariant sources of different widths. We choose the same parameters as in Ref. [10], namely “narrow” n ($\kappa = 0.21, N = 18$) and “wide” w ($\kappa = 0.191, N = 41$) sources. The derivative source is constructed by applying a covariant derivative to the wide source and is denoted as ∂_k , with $k = 1, 2, 3$.

C. Truncated Quark Propagator

We follow the procedure to remove an increasing amount of the lowest-lying Dirac eigenmodes and study the effect of this reduction on hadron masses. The truncated quark propagators take the form:

$$S_k(x, y) = S_{\text{FULL}}(x, y) - \sum_{i=1}^k \frac{1}{\lambda_i} v_i(x) v_i^\dagger(y). \quad (5)$$

Here $S_{\text{FULL}}(x, y)$ denotes the untruncated, $S_k(x, y)$ the truncated propagator, λ_i are the low-lying eigenvalues, $v_i(x)$ the eigenvectors and k the number of removed lowest modes. For instance, $k = 10$ means, that 10 low modes are removed from the quark propagator. We choose the truncation steps in the range $k = 2-30$, which corresponds to an eigenvalue cutoff between (8 – 180) MeV.

Figure 3: Mass evolution of $J = 1$ isovector mesons.Figure 4: Eigenvalues of $J = 2$ tensor mesons: (a) full case ($k = 0$), (b) after excluding $k = 30$ low modes in T_2 .

D. Meson Spectroscopy

Our analysis is based on the variational method, see Ref. [15–17]. The $J = 2$ interpolators from Table I fall into the irreducible representation E or T_2 of the hypercubic group O_h^4 . In addition, our interpolators \mathcal{O}_i fall into different irreducible representations of the parity-chiral and $SU(4)$ groups, as discussed in the previous chapter.

We construct the following cross-correlation matrices

$$C_{ij}(t) = \langle \mathcal{O}_i(t) \mathcal{O}_j^\dagger(0) \rangle, \quad (6)$$

and solve a generalized eigenvalue problem

$$C(t) \vec{v}_n(t, t_0) = \lambda_n(t, t_0) C(t_0) \vec{v}_n(t, t_0), \quad (7)$$

where $t_0 = 1$ is chosen as a reference timeslice in our analysis. From the solution of this eigenvalue problem we determine the energy levels of a given quantum channel. We choose time ranges where the eigenvalues $\lambda(t, t_0)$ decay exponentially, i.e.

$$\lambda^{(n)}(t, t_0) e^{-E_n(t-t_0)} (1 + \mathcal{O}(e^{-\Delta E_n(t-t_0)})), \quad (8)$$

⁴ For a mapping of the irreducible representations of O_h to the first few J numbers see Ref. [18]. The interpolators in E and T_2 representations are orthogonal, thus masses can be extracted separately.

and apply a one-exponential fit to extract masses E_n , where n labels the ground ($n = 1$) and excited ($n > 1$) states.

IV. RESULTS

As a consistency check we first extract masses of the isovector $J = 1$ mesons (ρ, ρ', a_1, b_1), Fig. 3, and compare them to the results shown in Refs. [1, 2], where propagators obtained within the JLQCD collaboration have been used. This comparison shows full agreement between both results.

In Fig. 4 we show the eigenvalues of the correlation matrix for all isovector tensor mesons before and after removal of the lowest 30 modes. While the eigenvalues are different for the different mesons in the untruncated case, they become identical in the truncated case. The degeneracy pattern is completely in line with the expectation from the $SU(4)$ symmetry, as discussed in Chapter II. Namely, the a_2 ($n = 1, 2$), ρ_2 ($n = 1$) and π_2 ($n = 1$) eigenvalues of the meson cross-correlators in T_2 become identical. The same holds true for the excited states of a_2 ($n = 3, 4$), ρ_2 ($n = 2$), π_2 ($n = 2$).

In Fig. 5 we show effective mass plots for all isovector mesons after truncation of the lowest Dirac modes. The quality of the plateau is worse than for the $J = 1$ states, where no derivative operators are used. This is why the error bars for the extracted masses are larger than for

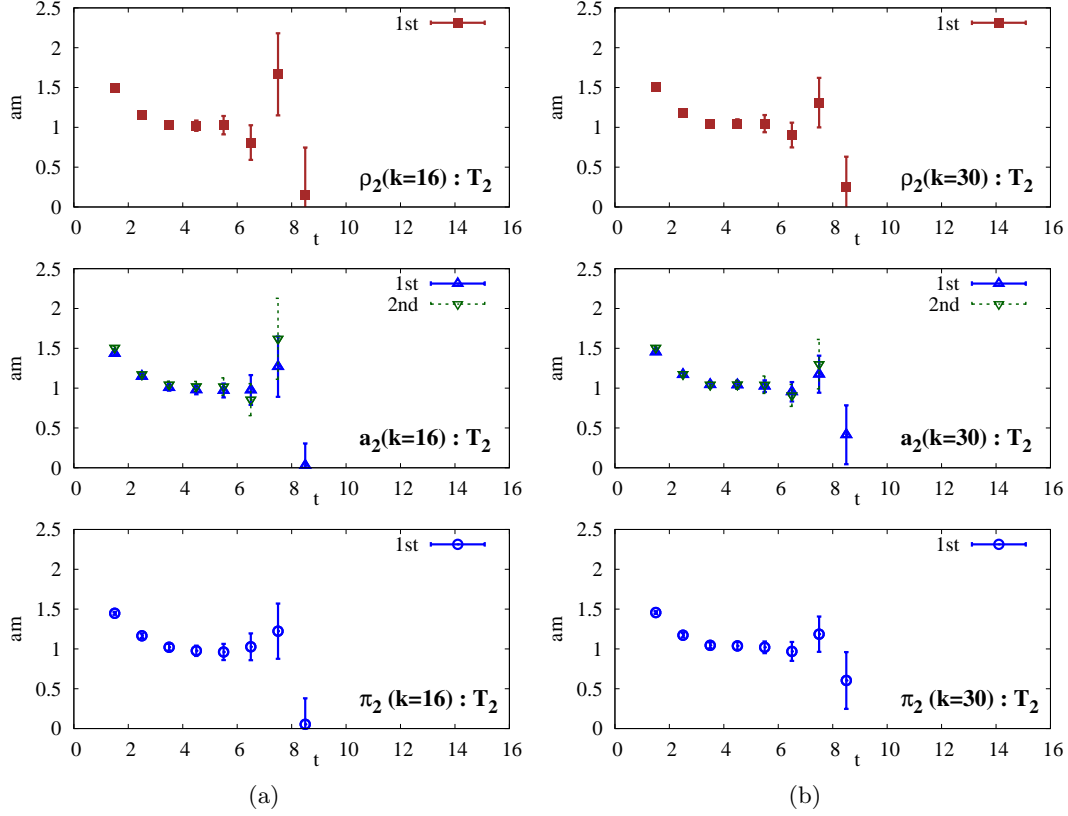


Figure 5: ρ_2 , a_2 , a'_2 , π_2 in T_2 : Effective masses after excluding (a) $k = 16$, (b) $k = 30$ low modes.

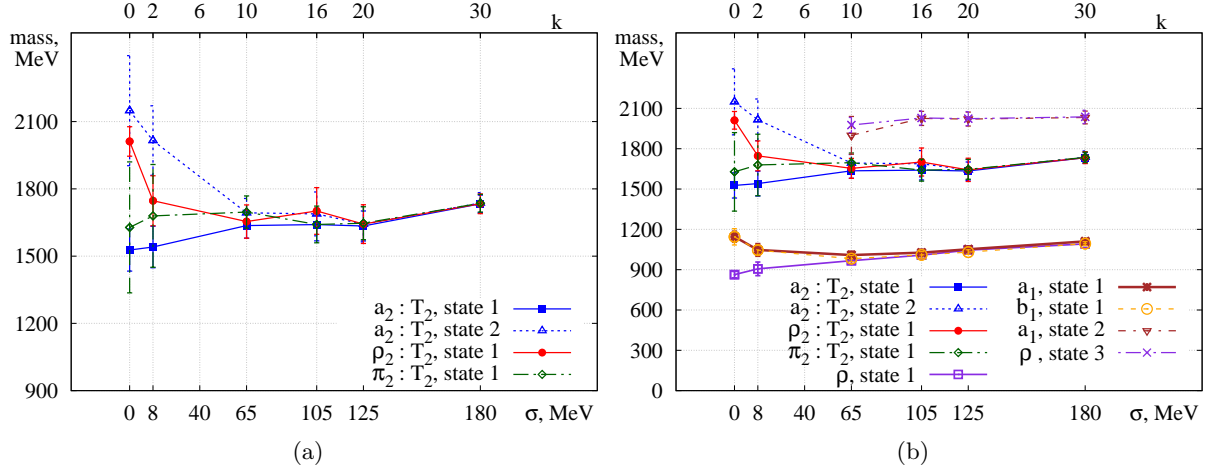


Figure 6: Ground state and excited state mass evolution of (a) $J = 2$ mesons in T_2 , (b) $J = 1$ and $J = 2$ mesons. The value k denotes the truncation step and σ the corresponding energy gap.

the $J = 1$ case. A comparison to the case of untruncated $J = 2$ mesons shows that the quality of the signal essentially improves after truncation, in line with our previous observations in Refs. [1–3]. The fit ranges and the extracted masses are given in Appendix A.

The final results for the masses of the two lowest a_2 states and the lowest states of π_2 and ρ_2 as a function of the truncation level are given in Fig. 6(a). We observe

a clear onset of the $SU(4)$ symmetry after elimination of the lowest 10 – 20 modes (truncation energy 65 – 125 MeV), in agreement with the respective results for the $J = 1$ isovector mesons shown in Fig. 3.

Finally, we compare in Fig. 6(b) the lowest energy level for $J = 2$ mesons with the lowest $J = 1$ energy level and its first excitation. No degeneracy is observed between the first excited $J = 1$ level and the ground $J = 2$ level.

However, to come to a definite conclusion we need much larger volumes: our small volume could affect in a different manner the $J = 1$ radially excited level and the ground $J = 2$ level.

V. SUMMARY AND CONCLUSIONS

We have studied the spin-2 isovector mesons upon removal of the lowest-lying Dirac eigenmodes from the valence quark propagators. Upon truncation of a small amount of the quasi-zero modes we have found the same $SU(4)$ symmetry pattern, as in our previous study of $J = 1$ mesons. This supports the existence of the $SU(4)$ symmetry in $J \geq 1$ mesons without the quasi-zero modes. This symmetry includes both the rotations of right- and left-handed quarks in the isospin space as well as rotations in the chiralspin space that mix the left- and right-handed components. This symmetry group implies the absence of the color-magnetic field in the system without the quasi-zero modes and might be interpreted as a mani-

festation of the dynamical color-electric string in QCD.

ACKNOWLEDGMENTS

We are grateful to S. Aoki, S. Hashimoto and T. Kaneko for their suggestion to use the JLQCD overlap gauge configurations and for their hospitality. We are very thankful to C. B. Lang for numerous discussions and help. Support from the Austrian Science Fund (FWF) through the grant P26627-N27 is acknowledged. The calculations have been performed on clusters at ZID at the University of Graz and at the Graz University of Technology.

Appendix A: Masses and Fits

Single exponential effective mass fits and corresponding $\chi^2/\text{d.o.f.}$ are presented in Table II for truncations $k = 0, 16, 20, 30$.

-
- [1] M. Denissenya, L. Y. Glozman and C. B. Lang, Phys. Rev. D **89**, 077502 (2014).
 - [2] M. Denissenya, L. Y. Glozman and C. B. Lang, Phys. Rev. D **91**, 034505 (2015).
 - [3] L. Y. Glozman, C. B. Lang and M. Schröck, Phys. Rev. D **86**, 014507 (2012).
 - [4] C. B. Lang and M. Schrock, Phys. Rev. D **84**, 087704 (2011).
 - [5] T. Banks and A. Casher, Nucl. Phys. B **169**, 103 (1980).
 - [6] L. Y. Glozman, Eur. Phys. J. A **51**, no. 3, (2015) 27.
 - [7] L. Y. Glozman and M. Pak, arXiv:1504.02323 [hep-lat].
 - [8] L. Y. Glozman, Phys. Lett. B **587**, 69 (2004).
 - [9] L. Y. Glozman, Phys. Rept. **444**, 1 (2007).
 - [10] G. P. Engel, C. B. Lang, M. Limmer, D. Mohler and A. Schafer, Phys. Rev. D **85**, 034508 (2012).
 - [11] S. Aoki *et al.* [JLQCD Collaboration], Phys. Rev. D **78**, 014508 (2008).
 - [12] S. Aoki *et al.* Prog. Theor. Exp. Phys. **2012**, 01A106 (2012).
 - [13] J. Noaki *et al.* [JLQCD and TWQCD Collaborations], Phys. Rev. Lett. **101**, 202004 (2008).
 - [14] T. Burch *et al.* [Bern-Graz-Regensburg Collaboration], Phys. Rev. D **70**, 054502 (2004).
 - [15] C. Michael, Nucl. Phys. B **259**, 58 (1985).
 - [16] M. Lüscher and U. Wolff, Nucl. Phys. B **339**, 222 (1990).
 - [17] B. Blossier *et al.*, JHEP **04**, 094 (2009).
 - [18] R. C. Johnson, Phys. Lett. B **114**, 147 (1982).

$k = 0$						$k = 16$					
state	n	am	$\chi^2/d.o.f$	t	i	state	n	am	$\chi^2/d.o.f$	t	i
$a_2 : T_2$	1	0.918 ± 0.056	6.28/5	3 - 9	2 4 6 8	$a_2 : T_2$	1	0.986 ± 0.044	0.84/3	4 - 8	2 4 6 8
	2	1.015 ± 0.059	0.64/2	4 - 7			2	1.292 ± 0.059	0.64/2	4 - 7	
$\rho_2 : T_2$	1	1.209 ± 0.040	1.24/2	2 - 5	2 4	$\rho_2 : T_2$	1	1.023 ± 0.063	0.82/2	4 - 7	2 4
$\pi_2 : T_2$	1	0.979 ± 0.176	0.19/2	4 - 7	6 8	$\pi_2 : T_2$	1	0.986 ± 0.049	0.69/3	4 - 8	6 8
$a_2 : E$	1	0.913 ± 0.078	0.37/2	4 - 7	2 8	$a_2 : E$	1	1.037 ± 0.039	4.02/3	4 - 8	2 8
$\rho_2 : E$	1	1.212 ± 0.034	2.80/3	2 - 6	8 10	$\rho_2 : E$	1	1.010 ± 0.031	1.84/4	3 - 8	8 10
$\rho : T_1$	1	0.519 ± 0.014	1.82/7	4 - 12	1 4 5 8	$\rho : T_1$	1	0.606 ± 0.014	1.38/5	6 - 12	1 4 5 8
	2	0.609 ± 0.013	4.55/7	4 - 12			2	0.928 ± 0.013	4.55/7	4 - 12	
$a_1 : T_1$	1	0.689 ± 0.023	4.25/3	3 - 7	1 4	$a_1 : T_1$	1	0.618 ± 0.012	1.50/4	5 - 10	1 4
$b_1 : T_1$	1	0.688 ± 0.036	2.11/3	3 - 7	22 25	$b_1 : T_1$	1	0.607 ± 0.015	3.70/5	4 - 10	22 25

$k = 20$						$k = 30$					
state	n	am	$\chi^2/d.o.f$	t	i	state	n	am	$\chi^2/d.o.f$	t	i
$a_2 : T_2$	1	0.982 ± 0.040	1.04/3	4 - 8	2 4 6 8	$a_2 : T_2$	1	1.042 ± 0.023	0.80/4	3 - 8	2 4 6 8
	2	1.044 ± 0.028	0.93/3	3 - 7			2	0.987 ± 0.028	0.93/3	3 - 7	
	3	1.459 ± 0.046	0.50/3	3 - 7			3	1.456 ± 0.046	0.50/3	3 - 7	
	4	1.507 ± 0.048	1.97/3	3 - 7			4	1.550 ± 0.048	1.97/3	3 - 7	
$\rho_2 : T_2$	1	0.987 ± 0.052	3.31/3	4 - 8	2 4	$\rho_2 : T_2$	1	1.042 ± 0.026	2.00/4	3 - 8	2 4
	2	1.502 ± 0.052	2.17/3	3 - 7			2	1.552 ± 0.052	2.17/3	3 - 7	
$\pi_2 : T_2$	1	0.990 ± 0.044	0.62/3	4 - 8	6 8	$\pi_2 : T_2$	1	1.043 ± 0.024	0.86/4	3 - 8	6 8
	2	1.477 ± 0.048	0.65/3	3 - 7			2	1.467 ± 0.048	0.65/3	3 - 7	
$a_2 : E$	1	1.044 ± 0.040	9.25/3	4 - 8	2 8	$a_2 : E$	1	1.053 ± 0.035	5.62/3	4 - 8	2 8
	2	1.138 ± 0.037	3.61/3	4 - 8			2	1.102 ± 0.037	3.61/3	4 - 8	
$\rho_2 : E$	1	1.029 ± 0.031	5.62/4	3 - 8	8 10	$\rho_2 : E$	1	1.047 ± 0.024	8.32/6	3 - 10	8 10
	2	1.466 ± 0.042	4.59/3	3 - 7			2	1.470 ± 0.042	4.59/3	3 - 7	
$\rho : T_1$	1	0.629 ± 0.011	4.87/5	5 - 11	1 4 5 8	$\rho : T_1$	1	0.657 ± 0.008	8.82/6	4 - 11	1 4 5 8
	2	0.669 ± 0.007	8.85/6	4 - 11			2	0.611 ± 0.007	8.85/6	4 - 11	
	3	1.224 ± 0.030	2.55/2	3 - 6			3	1.216 ± 0.030	2.55/2	3 - 6	
	4	1.245 ± 0.044	2.63/2	3 - 6			4	1.278 ± 0.044	2.63/2	3 - 6	
$a_1 : T_1$	1	0.632 ± 0.011	1.41/5	5 - 11	1 4	$a_1 : T_1$	1	0.668 ± 0.009	4.73/5	5 - 11	1 4
	2	1.222 ± 0.029	2.59/3	3 - 7			2	1.215 ± 0.029	2.59/3	3 - 7	
$b_1 : T_1$	1	0.620 ± 0.010	11.77/6	4 - 11	22 25	$b_1 : T_1$	1	0.657 ± 0.009	8.38/7	4 - 12	22 25
	2	1.240 ± 0.045	3.94/4	3 - 8			2	1.287 ± 0.045	3.94/4	3 - 8	

Table II: Results of fits to the eigenvalues at a truncation level $k = 0, 16, 20, 30$ for $J = 1, 2$ mesons. States are denoted by $n = 1, 2, \dots$. Corresponding mass values am are given in lattice units; t denotes the fit range and i labels the interpolators used in the construction of the cross-correlation matrix in a given quantum channel according to Ref. [10].